Albian-Maastrichtian stratigraphy of northern Chile between 28.5° and 30° S: record of early Andean orogenesis during the Cretaceous greenhouse world

Esteban Salazar[1,4*]; Christian Creixell[1]; Constantino Mpodozis[2]; Marcos Suarez[1]; Alfonso Rubilar[1]; Paula Castillo[3]; Andrés Folguera[4].

[1]Servicio Nacional de Geología y Minería, Av. Santa María 104, Providencia, Santiago, Chile.

[2]Antofagasta Minerals S.A., Avenida Apoquindo 4001, piso 18, Las Condes, Santiago, Chile.

[3]Institut für Geologie und Paläontologie, University of Münster, Germany.

[4]Universidad de Buenos Aires. Facultad de Ciencias Exactas y Naturales. Departamento de Ciencias Geológicas. Intendente Güiraldes 2160 (C1428EHA), Buenos Aires, Argentina.

[*]Corresponding author, esteban.salazar@sernageomin.cl

Christian Creixell: Christian.creixell@sernageomin.cl

Constantino Mpodozis: cochompodozis@gmail.com

Marcos Suarez: Marcos.suarez@sernageomin.cl

Alfonso Rubilar: Alfonso.rubilar@sernageomin.cl

Paula Castillo: paula.castillo@uni-muenster.de

Andrés Folguera: andresfolguera2@yahoo.com.ar

Abstract

The Late Cretaceous epoch was marked by significant climatic and tectonic events that shaped the evolution of the South American continental margin. In northern Chile, between 28.5° and 30° S, extensive sedimentary and volcanic sequences provide a crucial record of these processes. However, inconsistencies in stratigraphic nomenclature and the lack of precise chronological constraints have hindered a comprehensive understanding of this period. This study presents a revised stratigraphic framework for Upper Cretaceous units in the region, integrating recent geological mapping, U-Pb zircon dating, and new field observations. Three distinct north-south trending stratigraphic domains are identified, each characterized by unique sedimentary and volcanic successions linked to regional tectonic and climatic events. Four key evolutionary stages, from the Albian to the Maastrichtian, are revealed, including transitions between marine to continental sedimentation, phases of volcanic activity, and the development of retro-arc basins. Evidence of a previously undocumented marine transgression during the Turonian-Santonian interval suggests the influence of the global Late Cretaceous greenhouse event on sedimentation patterns in northern Chile. These findings highlight the complex interplay between tectonics, sedimentation, and climate during early Andean orogenesis. The revised stratigraphic framework provides a foundation for future geological studies in the region, improving correlations with adjacent areas and contributing to broader reconstructions of South America's geodynamic evolution during the Late Cretaceous.

Keywords: Cretaceous, Stratigraphy, Orogenesis, Paleoclimate

Estratigrafía del Albiano-Maastrichtiano del norte de Chile entre 28,5° y 30° S: registro de la orogenia andina temprana durante el mundo de invernadero del Cretácico. El Cretácico Tardío estuvo marcado por importantes eventos climáticos y tectónicos que modelaron la evolución del margen continental sudamericano. En el norte de Chile, entre los 28,5° y 30° S, extensas secuencias sedimentarias y volcánicas constituyen un registro clave de estos procesos. Sin embargo, las inconsistencias en la nomenclatura estratigráfica y la falta de un control cronológico preciso han dificultado una comprensión integral de este período. Este estudio presenta una revisión del marco estratigráfico para las unidades del Cretácico Superior en la región, integrando cartografía geológica reciente, dataciones U-Pb en circones y nuevas observaciones de terreno. Se identificaron tres dominios estratigráficos con rumbo norte–sur, cada uno caracterizado por sucesiones sedimentarias y volcánicas particulares, vinculados a eventos tectónicos y climáticos regionales. Se reconocieron cuatro etapas evolutivas principales, desde el Albiano hasta el Maastrichtiano, las que incluyen transiciones entre sedimentación marina y continental, fases de actividad volcánica y el desarrollo de cuencas de retroarco. Se destaca también evidencia de una transgresión marina previamente no documentada durante el Turoniano–Santoniano, lo cual sugiere influencia del evento global de efecto invernadero del Cretácico Tardío sobre los patrones de sedimentación en el norte de Chile. Estos resultados resaltan la compleja interacción entre tectónica, sedimentación y clima durante los inicios de la orogenia andina. El marco estratigráfico revisado proporciona una base para futuros estudios geológicos en la región, mejorando las correlaciones con áreas adyacentes y contribuyendo a

reconstrucciones más amplias de la evolución geodinámica de América del Sur durante el Cretácico Tardío.

Palabras Clave: Cretácico, Estratigrafía, Orogénesis, Paleoclima

1 Introduction

The Late Cretaceous epoch is marked by the occurrence of important geodynamic and climatic events on different scales. From a geodynamic perspective, the acceleration of the South Atlantic spreading ridge during the Early Cretaceous (Somoza and Ghidella, 2012; Granot *et al.*, 2015; Müller *et al.*, 2016) triggered major tectonic and paleogeographic transformations along the southwestern margin of South America, including: initial buildup of the Andean orogen (Mpodozis and Ramos, 1990), continentalization of the sedimentary environments (Aguirre-Urreta *et al.*, 2007), magmatic arc migration (Coira *et al.*, 1982; Folguera and Ramos, 2011), tectonic inversion of rift basins (Muñoz *et al.*, 2002; Salazar Pérez, 2012; Martínez *et al.*, 2012), and emplacement of important metallic ore deposits (Creixell *et al.*, 2020; del Real *et al.*, 2023). As for the climate, a global greenhouse event, with peak eustatic level in the Turonian (Haq and Huber, 2017), is vastly documented in the geological record around the world (Huber *et al.*, 2018). Nonetheless, evidence of the latter has yet to be documented in Chilean Andes stratigraphy.

The 28.5-30° S segment of the Chilean Andean orogen hosts a potential imprint of these and other events in the extensive Upper Cretaceous rock record; however, conclusive evidence has so far been hampered by a number of mismatches and uncertainties in the

present-day stratigraphic framework. The present study, therefore, presents a review of the Upper Cretaceous stratigraphy between 28.5° and 30° S. This is grounded in a critical analysis of the information contained in geological maps recently published by the Chilean Geological and Mining Service (Sernageomin), which include more than 50 U-Pb zircon ages on Cretaceous sequences (see Supplementary Table 1 for details), and new field observations, along with eight new U-Pb zircon ages. A new, coherent stratigraphic framework plus an updated regional geological map are thus presented. Three Upper Cretaceous stratigraphic domains are identified, each of which document regional events of tectonic and climatic nature. The results presented here are hoped to provide a solid basis for in-depth studies on the geological evolution of this period in this and other adjacent regions.

2 Geological framework

The study area encompasses the western (Chilean) flank of the Andean orogen in the southern Central Andes between 28.5 and 30° S (Fig. 1). This region is subdivided into two morphostructural domains: 1) The Frontal Cordillera to the east, characterized by thick-skinned tectonics, where Paleozoic to Triassic igneous basement blocks are reversely faulted over Meso-Cenozoic strata (Moscoso and Mpodozis, 1988), and 2) The Coastal Cordillera, where thin-skinned deformation dominates and exposes mainly Mesozoic strata (Moscoso and Mpodozis, 1988; Rodríguez *et al.*, 2015). Within the Coastal Cordillera domain, there are two N-S structural belts: western and eastern (Fig. 1). The western

Coastal Cordillera is dominated by a system of NNE-trending Early Cretaceous sinistral faults (Brown *et al.*, 1993; Emperán and Pineda, 2000; Welkner *et al.*, 2006; Arévalo *et al.*, 2009; Creixell *et al.*, 2012) with subsidiary normal and reverse faults, structures that expose Permian to Triassic sedimentary and metasedimentary units, Jurassic to Lower Cretaceous plutonic rocks, and minor volcanic strata. The eastern Coastal Cordillera presents superimposed thrust and normal faults affecting Upper Cretaceous units and penecontemporaneous plutonic complexes.

2.1 Pre-Upper Cretaceous stratigraphy

The oldest units in the studied segment are Carboniferous-Permian accretionary complexes cropping out in the western Coastal Cordillera (Bahlburg and Hervé, 1997; Willner *et al.*, 2008; Álvarez *et al.*, 2011; Creixell *et al.*, 2016, 2025). The contemporaneous magmatic arc is represented by plutonic complexes and coeval volcanic units of continental affinities cropping out in the westernmost block of the Frontal Cordillera, about 100 km inland (Nasi *et al.*, 1985; Mpodozis and Cornejo, 1988; Salazar *et al.*, 2013; Maksaev *et al.*, 2014; Ortiz and Merino, 2015; Murillo *et al.*, 2017) (Fig. 2), which is bounded to the west by the San Félix fault and southern equivalents, and to the east by the Pinte and La Punilla faults. Permian to Triassic arc-related igneous rocks crop out mostly to the east of the Carboniferous-Permian magmatic arc belt (Martin *et al.*, 1999; Oliveros *et al.*, 2018; González *et al.*, 2018; 2025; Salazar *et al.*, 2020) (Fig. 2).

During the Late Jurassic, continental volcanism and sedimentation was mainly developed in the Frontal Cordillera (Algarrobal and Lagunillas formations), whereas during the Early

Cretaceous it focused mostly on the Coastal Cordillera domain (Arqueros, Punta del Cobre, and Quebrada Marquesa formations) (Fig. 2). The Early Cretaceous activity was accompanied by marine carbonate sedimentation (Arqueros and Quebrada Marquesa formations, and Chañarcillo Group) (Emparán and Pineda, 1999; Arévalo *et al.*, 2009; Creixell *et al.*, 2013).

2.2 Upper Cretaceous stratigraphy

In the study area, the Upper Cretaceous stratigraphy has undergone several modifications over the past decades, mainly due to the incremental yet fragmented publication of geochronological data and new field and cartographic studies (Fig. 3). In the Coastal Cordillera, Albian-Cenomanian conglomerates and sandstones were defined by Emparán and Pineda (1999) as the Quebrada La Totora beds (here formalized as the Quebrada La Totora Formation) and assigned to the Checo de Cobre Member of the Cerrillos Formation (Arévalo *et al.*, 2009; Creixell *et al.*, 2013). Covering these sedimentary units, an andesitic volcanic succession was initially defined as the Viñita Formation (Aguirre and Egert, 1965; Emparán and Pineda, 1999), whereas north of 29.5° S, similar rocks were assigned to the Superior Member of the Cerrillos Formation (Arévalo *et al.*, 2009; Creixell *et al.*, 2013). However, the U-Pb zircon ages reported from the type locality of the Superior Member of the Cerrillos Formation (70-65 Ma; Maksaev *et al.*, 2009) differed from U-Pb zircon ages obtained for the volcanic succession (94-73 Ma; Arévalo *et al*., 2009; Creixell *et al*., 2013. Creixell *et al.* (2013) further subdivided this succession after the identification of an internal unconformity and assigned the upper part (78-84 Ma) to the Viñita Formation. Overlying

146 these volcanics, a thick succession of dacitic to rhyolitic tuffs and intercalated andesites was
147 defined as the Los Elquinos Formation (Aguirre and Egert, 1965), with an age between 71
148 and 65 Ma (Emparán and Pineda, 1999).

149 In the transition eastern part of the Coastal Cordillera and in the Frontal Cordillera, a red
150 siliciclastic unit that disconformably covers Upper Jurassic-Lower Cretaceous volcanic rocks
151 (Algarrobal Formation) was commonly assigned to the Pucalume Formation (Creixell *et al.*,
152 2013; Salazar *et al.*, 2013; Ortiz and Merino, 2015). A Coniacian-Santonian age was assigned
153 based on detrital zircon analysis and the maximum age of the overlying Viñita Formation
154 (Salazar Pérez, 2012; Creixell *et al.*, 2013). However, a U-Pb age of *ca.* 78 Ma from a tuff
155 next to the Pucalume Formation type section revealed that the unit originally defined as
156 Pucalume Formation was, in fact, younger than the Viñita Formation (Murillo *et al.* 2017;
157 Fig. 3). Hence, the Coniacian-Santonian red beds would correspond to a different and older
158 unit.

159 In the eastern Frontal Cordillera, Coniacian to Santonian red beds lie disconformably on
160 Upper Jurassic rocks of the Lagunillas Formation and are conformably covered by ca. 80 Ma
161 basaltic to andesitic volcanic rocks. These units were defined as the La Escondida (red beds)
162 and Las Yeguas (volcanics) members of the Manflas Formation (Salazar and Coloma, 2016).
163 Conformably over the Manflas Formation rocks, a thick succession of conglomerates, of late
164 Campanian-Maastrichtian age, was described by Salazar and Coloma (2016) under the name
165 of Valeriano Formation (Fig. 3).

2.3 Post-Upper Cretaceous stratigraphy

Paleocene and Eocene volcanic rocks unconformably cover Triassic, Jurassic, and Cretaceous units in the eastern border of the Coastal Cordillera and in the Frontal Cordillera (only Paleocene units shown in figure 2). These volcanics are usually associated with hypabyssal bodies related to an eastward migration of arc magmatism (Emparán and Pineda, 1999; Creixell et al., 2013; Salazar et al., 2013; Ortiz and Merino, 2015; Salazar and Coloma, 2016; Murillo et al., 2017). Finally, Miocene continental deposits are preserved in restricted intra-montane depocenters in the Frontal Cordillera (Rossel et al., 2016), while marine to continental deposits are exposed in valley lowlands and coasts along the Coastal Cordillera (Creixell *et al.*, 2012; Rodriguez *et al.*, 2015, 2018).

3 U-Pb geochronology

3.1 Methodology

Eight samples were collected for U-Pb zircon analysis: six tuffs and two sandstones (Supplementary Table 2). 1) Sample CS-08 belongs that an andesitic lapilli tuff intercalated between limestones of the topmost section of the Quebrada La Totora Formation in the Marquesa creek area. 2) Sample PLC-5 is a sandstone obtained from below the carbonate-bearing section at the top of Quebrada La Totora Formation in the Algarrobal ravine area. 3) Sample RAM-14 is an andesitic lapilli tuff collected from the upper section of the Quebrada Marquesa Formation at the Marquesa creek. 4) Sample EQS-12 is a welded dacitic tuff from the Quebrada Marquesa Formation along the Marquesa creek. 5) Sample EQS-04 was obtained from a dacitic vitric tuff collected near the type locality of the Los Elquinos Formation, in the Marquesa creek area. 6) Sample EQS-11 is a welded dacitic tuff northeast of the Condoriaco locality, in the footwall of the Vicuña fault and assigned to the Upper Cretaceous (*ca.* 85 Ma) Condoriaco Caldera unit by Emparán and Pineda (1999). 7) Sample KES-27 is an andesitic lapilli tuff collected from the Varillar locality at the base of the Las Yeguas Member. 8) Sample KES-31 is a sandstone also collected at the Varillar locality, cropping out just above the basal carbonate rocks of the La Escondida Member.

All samples were processed and analyzed at the Sernageomin laboratory. They were ground to particles smaller than 500 µm using Retsch equipment. Heavy minerals

were concentrated with a Gemini table and dense liquids. Zircons were separated manually under UV light, mounted in epoxy resin pucks (2.5 cm diameter), and polished to expose crystal interiors. Each sample included 30–120 zircons, depending on whether crystallization ages or detrital populations were analyzed. Temora 2 standards (417 Ma; Black *et al.*, 2004) were mounted alongside each sample.

Cathodoluminescence and backscattered electron imaging were used to identify internal structure, fractures and inclusions on the zircons. These analyses were obtained using a Zeiss EVO MA 10 scanning electron microscope equipped with a Gatan ChromaCL2 UV detector and Zeiss annular backscattered electron detectors. Laser ablation was conducted using a Photon Machines Analyte G2 193 nm excimer laser with a 30 µm spot size, a pulse frequency of 9 Hz, and an energy density of 2 mJ/cm², creating craters ~15–20 µm deep. Ablated material was transported via helium and argon gases to a Thermo Fisher Element XR mass spectrometer, where U, Th, and Pb isotopes were measured.

Data reduction was carried out with the Iolite software (Petrus and Kamber, 2012). Isotopic fractionation, instrumental drift, and sample position effects were corrected using the primary standard GJ-1 (609 Ma; Jackson *et al.*, 2004) and the Temora 2 standard. Secondary standards Mud Tank (732 Ma; Black and Gulson, 1978) and Plešovice (337 Ma; Sláma *et al.*, 2008) were used as quality controls. Common lead corrections were applied to $^{206}Pb/^{238}U$ ages using the ^{207}Pb method (Williams, 1998). Final ages were calculated and plotted using Isoplot (Ludwig, 2012). The decay constants and atomic ratios employed followed Steiger and Jäger (1977).

3.2 Results

The results for the eight samples analyzed are as follows (see figure 4 for age diagrams):

- CS-08 (andesitic lapilli tuff; Quebrada La Totora Formation): Forty-three zircons analyzed whose ages span from *ca.* 87 to 99 Ma. The age data depict a complex distribution deconvolved into three populations, the youngest of which (88.7±0.5 Ma) is interpreted as the closest to tuff deposition.
- PLC-5 (sandstone; Quebrada La Totora Formation): Sixty-three ages that vary from *ca.* 92 to 129 Ma. A clear, youngest population centered at 94.5±0.3 Ma is identified and interpreted as a maximum depositional age.
- RAM-14 (andesitic lapilli tuff; Quebrada Marquesa Formation): Sixty-six zircons analyzed, with sixty-five ages between *ca.* 104 and 111 Ma (average of 106.6±0.3 Ma) and one at *ca.* 95 Ma. Due to statistical significance, the first average is interpreted as the depositional age.
- EQS-12 (welded dacitic tuff; Quebrada Marquesa Formation): Sixty-five zircons analyzed, with ages normally distributed. The mean age of 108.5±0.3 Ma is interpreted as depositional age.
- EQS-04 (dacitic vitric tuff; Los Elquinos Formation): Thirty-nine zircons analyzed, which yield a unimodal distribution with a mean age of 76.1±0.3 Ma, along with a single younger zircon dated at *ca.* 57 Ma. Again, the main population is interpreted as depositional age.

- EQS-11 (welded dacitic tuff; Condoriaco Caldera): Sixty-eight zircons with a mean age of 53.6±0.2 Ma, which is considered its depositional age.
- KES-27 (andesitic lapilli tuff; Las Yeguas Member): Thirty-nine zircons analyzed, where the youngest population yielded an average age of 79.5±0.4 Ma (n=36), interpreted as depositional age.
- KES-31 (sandstone; La Escondida Member): Ninety-eight detrital zircons analyzed, with the youngest population at 86.2±0.9 Ma considered as the maximum depositional age. Additional age populations include Early Cretaceous, Late Jurassic, and minor Early Jurassic, Triassic, and Permian.

4 Proposal for a new Upper Cretaceous stratigraphy

Between 28.5° and 30° S, the cartographic and stratigraphic inconsistencies identified (Fig. 3) contrast with the abundant geochronological data and documented stratigraphic relationships available (Fig. 2). In this section, the need for a new regional, integrated stratigraphy for the Upper Cretaceous that both accounts for lateral facies variations and simplifies the nomenclature scheme is addressed.

Region-wide, east-west variations in the stratigraphy allow for three stratigraphic domains to be defined: Western, Central, and Eastern. The Western and Central domains are bounded by the Vicuña fault and its northern projection, whereas the Central and Eastern domains are bounded by an array of reverse west-verging faults that uplift Paleozoic basement blocks (Fig. 2).

4.1 Western Domain

The first-order feature of the Western Domain can be considered the eastern limb of a wide north-south monocline structure, with subhorizontal Upper Jurassic-Lower Cretaceous units to the west and east-dipping Upper Cretaceous units to the east. Second-order normal and reverse faults and folds are nested within the first-order structure. Within the monoclinal geometry, the dips decrease up-section from the Albian Quebrada Marquesa Formation to Campanian-Maastrichtian volcanics of the Higuera beds (see below) at the top. The Albian-Maastrichtian stratigraphic record is almost continuous in this domain, although minor local unconformities are present. The representative stratigraphic column of the Western Domain is described below.

4.1.1 Quebrada la Totora Formation (105-88 Ma)

Defined along the Marquesa creek (Emparán and Pineda, 1999; Fig. 2), it corresponds to a sedimentary succession composed of conglomerates, sandstones, and limestones, with intercalations of andesitic to rhyolitic lavas and tuffs. At its type locality, it overlies Albian pyroclastic rocks of the Quebrada Marquesa Formation, while in the Algarrobal ravine and north of the Huasco River it covers carbonated rocks of the Chañarcillo Group (Valanginian-Aptian; Arévalo *et al.*, 2009). A strong lateral facies variation was identified in the upper section of this formation around the Palo Plantado ravine area (Fig. 2), where it is composed almost entirely of andesitic volcanics with only minor intercalations of conglomerates, sandstones and dacitic lava domes and tuffs (Creixell *et al*., 2013) ("v" facies in figure 2).

The Quebrada La Totora Formation reaches up to 1,700 m in thickness in the Algarrobal ravine (Fig. 5), where it consists of clast-supported conglomerates intercalated with red bioturbated sandstones with pedogenetic carbonate and mud cracks, heterolithic sandstones, cross- and flat-bedded yellow sandstones, a ~40 m-thick laminated limestone at the top (yellow swath in figure 6A), and minor intercalations of andesitic tuffs throughout. At the Marquesa creek, the formation comprises, from bottom to top, 150 m of clast-supported coarse conglomerates, 150 m of red bioturbated sandstones with paleosols, 80 m of planar and cross-laminated heterolithic sandstones, and 70 m of limestones; of which the last includes laminated mudstones and wackestones, cross-laminated grainstones, chert, and an andesitic lapilli tuff intercalated near the top (yellow swath in figure 6B).

Two U-Pb zircon ages from the underlying Quebrada Marquesa Formation obtained in this study (106.6±0.3 Ma, sample RAM-14; 108.5±0.3 Ma; sample EQS-12), represent an upper boundary (i.e., maximum depositional age) for the Quebrada La Totora Formation. In the sedimentary facies of this formation ("s" facies in figure 2), an intercalated tuff yielded an age of 98±1 Ma, whereas five U-Pb ages between 89 and 94 Ma were reported from volcanic facies of the formation (Creixell *et al.*, 2013). In addition, the present study reports a U-Pb age of 88.7±0.5 Ma (sample CS-08) from an andesitic lapilli tuff interbedded with carbonate sediments near the top of the section at Marquesa creek (Figs. 4 and 6B), and a maximum depositional age of 94.5±0.3 Ma (sample PLC-5) from a sandstone below carbonate strata at the top of

the Algarrobal ravine section (Figs. 4 and 6A). Collectively, these ages allow assigning a depositional age between 105 and 88 Ma for the Quebrada La Totora Formation.

4.1.2 Los Elquinos Formation (88-76 Ma)

This formation was defined in the upper part of the Marquesa creek as a succession of dacitic to rhyolitic volcanic rocks, conformably covering the Viñita Formation (Aguirre and Egert, 1965; Emparán and Pineda, 1999). In this study, the Viñita Formation andesites are included within the Los Elquinos Formation based on stratigraphic continuity and lithological and geochronological evidence. In terms of distribution, the Los Elquinos Formation extends continuously north of its type locality, unconformably overlying both the sedimentary and volcanic facies of the Quebrada La Totora Formation (Fig. 2).

At its type locality, the base is composed of 400 m of hyaloclastite andesitic lavas and lapilli tuffs. Its middle section consists of 1,400 m of vitric, occasionally welded, dacitic tuffs, andesitic to dacitic lavas, and polymictic and monomictic volcanic breccias, with abundant basaltic andesite dykes and sills; facies that are well exposed within and around a caldera-like structure north of the Condoriaco locality (Emparán and Pineda, 1999). The topmost 300 m is made of basaltic andesite and andesite volcanics (Fig. 5).

Four U-Pb ages have been reported for this formation, ranging from 78 to 85 Ma (Emparán and Pineda, 1999; Creixell *et al.*, 2013) (Fig. 2). In this study, a new U-Pb zircon age of 76.1±0.3 Ma was obtained from a dacitic vitric tuff sampled near its

type locality (Figs. 2 and 4). The age of this formation is therefore bracketed to between 88 and 76 Ma.

4.1.3 Higuera beds (76-69 Ma)

Defined in this work, it refers to a 1,300 m-thick intermediate to felsic volcanic succession, mainly pyroclastic, outcropping only in the northern part of the study area along the Huasco River (Fig. 2). It unconformably covers *ca.* 80 Ma volcanics corresponding to the Los Elquinos and Las Yeguas rocks (Fig. 2). This unit includes felsic lapilli and ash tuffs, andesitic lavas and sills, and localized, massive clast-supported conglomerates. A U-Pb zircon age of *ca.* 74 has been reported in the Huasco river valley (Arévalo *et al.*, 2009). As this unit is intruded by *ca.* 69 Ma plutons, its age can be constrained to 76-69 Ma.

4.2 Central Domain

This domain exposes a west-dipping succession of Turonian to Paleocene strata, typically intruded by Eocene plutons. The beds are internally affected by second-order, doubly vergent reverse faults and related folding. The boundaries of this domain are well defined in the Elqui Valley by the Vicuña fault to the west and by west-verging basement faults to the east (Fig. 2). However, further north, its western boundary is marked by an array of west-verging reverse faults and its eastern margin by the Las Pircas basement fault (Fig. 2). The representative stratigraphic column of the Central Domain is detailed below.

4.2.1 La Escondida Formation (92-80 Ma)

In this study, the La Escondida Member of the Manflas Formation (Salazar and Coloma, 2016) is elevated to formation rank (Fig. 3). This unit corresponds to a red siliciclastic succession that disconformably covers a rough paleotopography carved in the Upper Jurassic-Lower Cretaceous Algarrobal Formation, as evidenced by onlap relationships (Fig. 6C), and is, in general, conformably covered by the Las Yeguas Formation (see below). In the north, around the El Tabaco ravine, it covers in angular unconformity Valanginian volcanics and reaches 550 m in thickness. There, it is dominated by heterolithic sandstones and includes crinoid-bearing carbonate rocks at its base (*Isselicrinus*? sp.; Fig. 6F). In the El Carrizo locality this unit reaches approximately 1,000 m in thickness, with conglomerates capped by calcareous siltstone at its base, and sandstones with abundant heterolithic bedding structures towards the top (Fig. 5). Further south, along the Turbio River and covering 70 m of conglomerates of the Algarrobal Formation, this unit comprises 12 m of carbonated siltstone at its base and 400 m of lithic fine- to medium-grained sandstones with minor intercalations of lavas and conglomerates (Fig. 5). The sandstones show tractive and heterolithic structures, convolute bedding, normally graded conglomerate lenses, and an intercalated hyaloclastite wedge that laterally varies to a peperitic basaltic andesite lava flow (Fig. 5).

Two published detrital zircon analyses near the Carrizo locality derived maximum depositional ages of *ca.* 92 and 89 Ma (Creixell *et al.*, 2013). Additionally, a maximum depositional age of 86.2±0.9 Ma was obtained in this study from a sandstone at the

Varillar locality (Figs. 4 and 6D). Six igneous U-Pb ages closely grouped between 80-82 Ma of the overlying Las Yeguas Formation reported along this domain constrain its minimum depositional age (Creixell *et al.*, 2013; Salazar *et al.*, 2013; Ortiz and Merino, 2015; Murillo *et al.*, 2017; this study). However, an older 84 Ma age reported by Murillo *et al.* (2017) just north of the Varillar locality may suggest a gradational contact between the La Escondida and Las Yeguas formations in some places. The depositional age of La Escondida is therefore considered as Turonian-early Campanian (Fig. 2).

4.2.2 Las Yeguas Formation (84-80 Ma)

In this work, the Las Yeguas Member of the Manflas Formation (Salazar and Coloma, 2016) is elevated to formation rank (Fig. 3). In the southern part of the study area, at the Varillar locality, this formation consists of 300 m of andesitic lapilli tuffs and lavas, and it conformably covers the La Escondida Formation (Fig. 5). Further north, west of the El Carrizo locality, it is also composed of andesitic lavas and tuffs, but it covers the La Escondida Formation in an angular unconformity. Seven published U-Pb zircon ages in this domain range between 84 and 80 Ma (Fig. 2). In the present contribution, a basal andesitic lapilli tuff at Varillar yielded a U-Pb age of 79.5±0.4 Ma (Fig. 4). This suggests a late Santonian-early Campanian age range for this formation.

4.2.3 Pucalume Formation (78-69 Ma)

Defined in the southern part of the study area (Dediós, 1967; Fig. 2), this unit is composed of 200 to 800 m of conglomerates, sandstones, tuffs, and lavas resting

disconformably on Permian–Triassic units at its type locality, and on the Las Yeguas Formation at the Carrizo and Varillar localities (Emparán and Pineda, 1999; Salazar *et al.*, 2013; Murillo *et al.*, 2017) (Figs. 2 and 6E). In the northern part of the study area a small succession is preserved in the footwall of the San Félix fault (Fig. 2). Published U-Pb zircon ages in this formation include 77.6±0.7 Ma from an intercalated tuff and 74 and 69 Ma maximum depositional ages from detrital zircons, all of them around the type locality (Murillo *et al.*, 2017). In addition, a 72.1±2.1 Ma age from a lapilli tuff intercalated within sandstones in the footwall of the San Félix fault was obtained by Salazar *et al*. (2013). The age of this formation is therefore constrained between 78 and 69 Ma.

4.3 Eastern Domain

Unlike the previous two domains, Upper Cretaceous units in the Eastern Domain are preserved in sparse and discontinuous areas, lying paraconformably on Upper Jurassic units (Fig. 2). Turonian to lower Campanian units (La Escondida and Las Yeguas formations) outcrop only in the northernmost part of the domain (Manflas River area), whereas upper Campanian-Maastrichtian strata (Valeriano Formation) crop out more widely, normally at the footwall of east-verging basement faults (Fig. 2). The most relevant formations are explained below.

4.3.1 La Escondida Formation (94-80 Ma)

This unit crops out in the Manflas and Valeriano river areas (Fig. 2), where it was formerly defined as the La Escondida Member (Salazar and Coloma, 2016; Fig. 3). In the Eastern Domain, it disconformably overlies the Upper Jurassic Lagunillas

Formation and is gradationally covered by the Las Yeguas Formation (Fig. 5). The unit consists of up to 120 m of sandstones with trough and epsilon cross-bedding, fine-grained conglomerates, and fine-grained sandstones rich in pedogenetic carbonate levels. Maximum depositional ages from detrital zircon analysis of *ca*. 90 and 94 Ma, and Ar/Ar groundmass dating of the overlying Las Yeguas Formation (*ca.* 80 Ma) constrain the deposition of this unit in the Eastern Domain between the Turonian and early Campanian (Salazar and Coloma, 2016).

4.3.2 Las Yeguas Formation (86-80 Ma)

In the Eastern Domain, the Las Yeguas Formation crops out only in the Manflas River area (Fig. 2). It consists of approximately 100 m of andesitic to basaltic andesite lavas, with volcaniclastic intercalations to the west, lying in gradational contact over the La Escondida Formation and conformably covered by the Valeriano Formation. Geochemically, these lavas show a high-K, calc-alkaline signature with a few slightly alkaline basalts (Salazar and Coloma, 2016). U-Pb detrital zircon analysis from an intercalated sandstone shows a maximum depositional age of 85.5±1.3 Ma (Merino *et al*., 2013; Fig. 2). In consideration of a reported Ar/Ar groundmass age of *ca.* 80 Ma (Salazar and Coloma, 2016), a Santonian-early Campanian age can be assigned for this unit.

4.3.3 Valeriano Formation (75-68 Ma)

It is defined in the northern part of the study area, along the eponymous river, where it consists of a 1,000 m-thick retrograding clastic (sandstones and conglomerates) succession interpreted as alluvial and fluvial deposits with rare tuff intercalations

(Fig. 5). It occurs in the footwall of a series of east-verging basement faults (Valeriano, La Plata, and Apolinario faults; Fig. 2). At its type locality, it conformably covers the Las Yeguas Formation (Salazar and Coloma, 2016). Further south, it also consists of retrograding conglomerates and sandstones, lying disconformably over Upper Jurassic Lagunillas Formation rocks (Fig. 2). A U-Pb zircon age of *ca.* 75 Ma from an ash tuff reported near its base by Salazar and Coloma (2016), and three detrital zircon maximum depositional ages of 94, 83, and 68 Ma (Merino *et al.*, 2013; Salazar and Coloma, 2016; Murillo *et al.*, 2017) indicate a late Campanian-Maastrichtian age for the Valeriano Formation.

5 Discussion

The revised Upper Cretaceous stratigraphy for the 28.5-30° S segment is presented in figure 7, whereas the relative locations of the magmatic arcs and the different depocenters are plotted in figure 8. Four paleogeographic stages are suggested and detailed below.

5.1 Late Albian-Cenomanian: Clastic deposition in an intra-arc basin

Upper Albian-Cenomanian strata (Quebrada La Totora Formation) occur exclusively in the Western Domain and consist of clastic sediments that include scarce andesitic volcanics. No deposition is recorded for the Central and Eastern domains during this period. In the Central Domain, the Turonian La Escondida Formation disconformably onlaps paleovalley slopes eroded in concordant Upper Jurassic-Lower Cretaceous volcanics (Algarrobal Formation), generating progressive thickness changes (Fig. 6C).

This rough topography could have been due to a base-level drop followed by a relative base-level rise prior to the deposition of carbonates and siliciclastic sediments of the La Escondida Formation. In the Eastern Domain, this formation rests paraconformably on Upper Jurassic rocks (Lagunillas Formation). These features suggest that, during the Late Albian-Cenomanian, the Western Domain remained subject to clastic sediment aggradation below a regional base level, hosting discrete volcanism, whereas the Central and Eastern domains remained as topographic highs with no accommodation space generated (Figs. 7 and 8). The deep paleovalleys carved in the Central Domain may represent the topographic front of this paleohigh.

The Quebrada La Totora Formation covers and is covered by thousands of meters of intra-arc volcanic successions (Fig. 7). These volcanic rocks show evidence of accommodation via normal fault systems related to volcanotectonic depressions (Emparán and Pineda, 1999; Arévalo *et al.*, 2009; Creixell *et al.*, 2013). Regional equivalents to the Quebrada La Totora Formation have been recognized around 27.5° S, as part of the Cerrillos Formation (Maksaev *et al.,* 2009), and at 33° S, as part of the Las Chilcas Formation (Boyce *et al.*, 2020), suggesting regional-scale controls on sediment accumulation and preservation (Fig. 9). Previous authors have interpreted the tectonic settings of these clastic deposits and their regional equivalents as foreland basins (Maksaev *et al.*, 2009; Boyce *et al.* 2020), with alternative interpretations including the filling of an extensional rift basin (Arévalo, 2009) and post-rift sedimentation (Martínez *et al.*, 2013). However, all these

possibilities seem inconsistent with the intra-arc setting suggested here (Fig. 8). The causes of this persistent depositional feature recognized along >600 km in the intra-arc domain of the Late Cretaceous are unknown; some alternatives could be an increase in sediment accommodation and supply due to tectonic or climatic triggers and/or a relative decrease in volcanic activity.

From a tectonic perspective, the shift from Early Cretaceous marine sedimentation (Quebrada Marquesa Formation) to fluvio-alluvial deposition during the late Albian-Cenomanian reflects the continentalization of the margin (Fig. 9). This continentalization took place during a period of global eustatic rise (Haq, 2014; Fig. 10), which suggests a tectonic uplift of the continental margin during the Albian. The tectonic mechanism responsible for this uplift has not been documented in the surface geology of the margin; however, it roughly coincides with a sudden ~40 mm/yr increase in the spreading rate of the South Atlantic and the consequent westward motion of the South American plate around 120 Ma (Müller *et al.*, 2016). From a climatic perspective, ocean temperatures obtained from isotopic signatures on benthic and planktonic foraminifera in the Pacific, Atlantic, and Indian oceans depict a warming event between the Albian and the Turonian, with peak temperatures in the Cenomanian-Turonian, and rapid cooling in the Campanian-Maastrichtian (Friedrich *et al.*, 2012; Huber *et al.*, 2018) (Fig. 10). As global warming has a strong influence on the occurrence of large precipitation events and, consequently, on fluvial transport enhancement (Goudie, 2006; Foreman *et al.*,

2012; Bataille *et al.*, 2019), a possible climate control on sediment supply rates within the intra-arc basin during the Albian-Cenomanian is suggested.

5.2 Turonian-Santonian: Onset of retro-arc sedimentation and the Cretaceous Thermal Maximum

During the Turonian, clastic deposition occurred throughout the study area (Fig. 7). In the Western Domain, the Quebrada La Totora Formation records a shift from clastic to carbonate deposition at the Algarrobal ravine and the Marquesa creek (Fig. 5). In the Central Domain, the Turonian is marked by the onset of sedimentary deposition filling deep paleovalleys carved in the Upper Jurassic-Lower Cretaceous Algarrobal Formation (Fig. 6C). It begins with a few meters of carbonate mudstones and bioclastic packstones carrying columns of crinoids (*Isselicrinus*? sp.), followed by subaqueous heterolithic sandstones, with fine conglomerates and tuffites at the top (Fig. 5). The Eastern Domain is marked by mudstones with paleosol structures and trough cross-bedded sandstones and conglomerates, representing overbanks and channel-belt facies within a fluvial depositional environment (Salazar and Coloma, 2016).

The crinoid fossils reported in the La Escondida Formation (Fig. 6F) have significant paleoenvironmental implications. Specifically, the genus *Isselicrinus* Rovereto, 1914 is known from the Late Cretaceous to the Miocene. It attained a worldwide distribution during the Eocene (Roux et al., 2024), in calm offshore environments below storm-wave and soft-bottom substrate, especially on upper bathyal slopes (Roux et al. 2006; Engelke et al., 2016). They were fully marine (stenohaline) and

lived as stalked, fixosessile, epifaunal suspension feeders. Their presence in the Turonian levels of the La Escondida Formation in the Central Domain, provides evidence of an undocumented marine transgression in northern Chile. A major Cenomanian-Turonian transgression has also been identified in forearc and retro-arc positions in the Andes of Peru and Ecuador by Jaillard *et al.* (2005), who interpreted it as a consequence of a global eustatic maximum in a compressional tectonic context. The global eustatic maximum during the Turonian reached more than 250 m above the present sea level (Haq, 2014; Figs. 10 and 11) and has been attributed to a greenhouse event (Friedrich *et al.*, 2012; Wang *et al.,* 2014; Huber *et al.*, 2018) globally referred to as the Cretaceous Thermal Maximum (CTM; Clarke and Jenkyns, 1999). The Turonian carbonates identified at the base of the La Escondida Formation could be the very first record of the CTM recognized in northern Chile.

Although Turonian-Coniacian carbonates at the top of the Quebrada La Totora Formation in the Western Domain (Fig. 5) have not yet provided direct evidence of a marine environment, they are most likely related to the Turonian marine transgression (Fig. 10). Marine incursion should have thus come from the west, involving both the Western and Central domains but not the Eastern Domain. This suggests the presence of a topographic barrier between the Central and Eastern domains. The latter was already suggested by Merino *et al.* (2013) based on the presence of Late Jurassic, Carboniferous and Permian detrital zircons in both domains of the La Escondida Formation, most likely sourced from the westernmost basement block of the Frontal Cordillera (Fig. 2). This basement block is uplifted by

a bi-vergent reverse fault system, suggesting possible thick-skinned compressional tectonics in the area at least since the Turonian. South of the study area (Elqui Valley), Lossada *et al.* (2017), based on thermochronology, did not find significant pre-Eocene exhumation events, although it cannot be discarded that Cretaceous (or earlier) signals had been reset due to magmatic activity.

At a more regional scale, Turonian carbonates have been discontinuously documented at the top of mid-Cretaceous clastic continental units between 27.5° and 33° S (Fig. 9). Some of these present unidentified gastropods (Segerstrom and Parker, 1959; Aguirre and Egert, 1965), whereas those at around 33° S carry marine fossils (Rivano *et al.*, 1993; Wall *et al.*, 1999; Tunik and Álvarez, 2008). The discontinuous spatial distribution of Turonian marine carbonates along this segment may result either from local erosion or from a highly irregular paleoshoreline featuring discrete marine inlets.

5.3 Early Campanian: The Las Yeguas volcanism

At approximately 80 Ma, basaltic andesite to dacitic lavas were extruded in the three stratigraphic domains (Fig. 7). In the Western Domain (intra-arc setting) these products mingle within a pile of nearly 3,000 m of volcanics of the Los Elquinos Formation (88-76 Ma). However, further east, in the Central and Eastern domains, these lavas (Las Yeguas Formation) constituted a particular event, lasting roughly 1-4 Myr (Figs. 7 and 8). Occurring within a retro-arc environment (Fig. 8), neither the cause nor the nature of this off-arc magmatism are well understood; however, similar high-K calc-alkaline to alkaline signatures have been recognized between 32°

and 42° S in retro-arc products related to the subduction of the Farallon-Aluk ridge during the latest Cretaceous (Iannelli *et al.*, 2020). It is likely that the subduction of such a spreading ridge at the studied latitudes at around 80 Ma (Fig. 12) could have been the cause of the Las Yeguas volcanism.

5.4 Late Campanian-Maastrichtian: Intermediate to felsic arc magmatism and foreland sedimentation

In the Western Domain, this period is marked by the accumulation of a 1.3 km-thick succession of felsic pyroclastics (Higuera beds) and andesitic lavas in an intra-arc basin, outcropping in the northernmost part of the studied segment (Fig. 2), and contemporaneous intrusives emplaced in the Los Elquinos Formation, south of 29° S (Emparán and Pineda, 1999; Creixell *et al.*, 2013). These differences in exposure could be due to tectonic reasons: the Higuera beds are located in the footwall of the Agua de los Burros fault (Fig. 2), whereas in the south the intrusives are uplifted by the Las Cañas fault. These plutons are unconformably covered by *ca.* 54 Ma Ypresian volcanics (Emparán and Pineda, 1999), evidencing Maastrichtian-Paleocene activity of the Las Cañas fault.

In the Central Domain, clastic deposition (Pucalume Formation) took place in a continental alluvial setting with frequent volcanic activity. At the Varillar locality these deposits seal a reverse basement fault affecting Campanian volcanics (Fig. 2), evidencing tectonic uplift within this domain in Campanian-Maastrichtian times. Consistently, detrital zircon age data indicate source regions from an uplifted Carboniferous-Permian basement block to the east (Murillo *et al.*, 2017). Further

east, clastic deposition (Valeriano Formation) took place in isolated, syntectonic depocenters in the footwall of major basement faults (e.g., La Plata, Apolinario, Valeriano), with detrital zircon data showing a strong provenance from uplifted Permian-Triassic basement blocks (Ortiz and Merino, 2015; Salazar and Coloma, 2016; Murillo *et al*., 2017). During this period, tectonic blocks bounded by reverse faults in the three stratigraphic domains show evidence of uplift via erosional processes, suggesting a possible compressional tectonic activity.

6 Conclusions

The study of Upper Cretaceous stratigraphy in northern Chile, between 28.5 and 30° S, has established three north-south trending stratigraphic domains and provided a regional framework for paleogeographic evolution. Four key stages in sedimentary and tectonic development are identified.

During the late Albian-Cenomanian stage, clastic deposition with scarce volcanic input (Quebrada La Totora Formation) predominated in the Western intra-arc basin domain, while the Central and Eastern domains remained as topographic highs with no accommodation space generated. This phase of continentalization of the margin, marked by a shift from marine (Aptian) to fluvio-alluvial sedimentation (Albian), coincides with a progressive global ocean temperature and sea level rise, of which a possible tectonic uplift of the continental margin can be inferred, with its mechanisms yet to be identified. Climatic and eustatic controls over sediment supply rates and accommodation during this stage remain open.

The Turonian-Santonian phase is marked by widespread deposition across all three domains. The La Escondida Formation represents the first Upper Cretaceous unit in the Central and Eastern domains, featuring marine carbonates with crinoid fossils at its base in the Central Domain, indicating a previously undocumented Turonian marine transgression. This event likely resulted from a global eustatic maximum associated with the Cretaceous Thermal Maximum. In the Western Domain, carbonate deposition was followed by arc-related volcanism (Los Elquinos Formation), while the Eastern Domain remained continental. The transgression's limited eastward reach implies the presence of a topographic barrier, likely associated with uplifted tectonic blocks.

The Campanian stage is characterized by retro-arc volcanic activity represented by the Las Yeguas Formation in the Central and Eastern domains, partly contemporaneous to the arc-related Los Elquinos Formation in the Western Domain. These volcanic incursions towards the retro-arc province coincide temporally with the subduction of the Aluk-Farallon oceanic ridge in the studied segment.

During Campanian-Maastrichtian, pyroclastic deposition took place in the Western Domain (Higuera beds), along with clastic and volcaniclastic sedimentation (Pucalume Formation) and reverse faulting in the Central Domain. The Eastern Domain developed isolated clastic depocenters (Valeriano Formation) filled with eroded material from reversely uplifted basement blocks.

The updated stratigraphic framework for the Upper Cretaceous presented here highlights the possible coexistence of extensional and compressional regimes across distinct domains, and underscores the importance of integrating greenhouse climate data into future tectono-sedimentary interpretations for Cretaceous basins in northern Chile.

7 Acknowledgements

This work was funded by the Plan Nacional de Geología program of the Chilean Geological and Mining Service (Servicio Nacional de Geología y Minería - Sernageomin). We would like to thank all laboratory staff involved in sample preparation processes. Also Leonardo Córdova, for his help in getting the manuscript formatted for submission. And the colleagues R. Merino, J. Álvarez, I. Murillo, D. Villela, R. Ferrando, and A. Echaurren for sharing their insights on Cretaceous stratigraphy in northern Chile. Special thanks to paleontologists M. Salamon and P. Gorzelak, for their discussions on Crinoidea systematics. Thorough reviews by Matías Barrionuevo, Alfonso Encinas, Felipe Tapia, and Maisa Tunik, and editorial handling by Daniel Bertin, greatly improved this manuscript.

8 References

Aguirre Le Bert, L.; Egert R., E. 1965. Cuadrángulo Quebrada Marquesa, Provincia de Coquimbo. Instituto de Investigaciones Geológicas, Carta Geológica de Chile 15: 92 p., 1 mapa escala 1:50.000. Santiago.

Aguirre-Urreta, M.B.; Mourgues, F.A.; Rawson, P.F.; Bulot, L.G.; Jaillard, E. 2007. The Lower Cretaceous Chañarcillo and Neuquén Andean basins: ammonoid biostratigraphy and correlations. Geological Journal 42(2): 143-173. https://doi.org/10.1002/gj.1068

Álvarez, J.; Mpodozis, C.; Arriagada, C.; Astini, R.; Morata, D.; Salazar, E.; Valencia, V.; Vervoort, J.D. 2011. Detrital zircons from late Paleozoic accretionary complexes in north-central Chile (28-32 °S): possible fingerprints of the Chilenia terrane. Journal of South American Earth Sciences 32(4): 460-476. https://doi.org/10.1016/j.jsames.2011.06.002

Arévalo, C.; Mourgues, F.; Chávez, R. 2009. Geología del área Vallenar-Domeyko, Región de Atacama. Servicio Nacional de Geología y Minería, Carta Geológica de Chile, Serie Geología Básica 120: 64 p., 1 mapa escala 1:100.000. Santiago.

Bahlburg, H.; Hervé, F. 1997. Geodynamic evolution and tectonostratigraphic terranes of northwestern Argentina and northern Chile. Geological Society of America Bulletin 109 (7): 869-884. https://doi.org/10.1130/0016-7606(1997)109<0869:GEATTO>2.3.CO;2

Bataille, C. P.; Ridgway, K. D.; Colliver, L.; Liu, X. M. 2019. Early Paleogene fluvial regime shift in response to global warming: A subtropical record from the Tornillo Basin, west Texas, USA. *Bulletin*, *131*(1-2), 299-317.

Boyce, D.; Charrier, R.; Farías, M. 2020. The first Andean compressive tectonic phase: sedimentologic and structural analysis of mid-Cretaceous deposits in the Coastal Cordillera, central Chile (32°50′ S). Tectonics 39(2): e2019TC005825.

Brown, M.; Diaz, F.; Grocott, J. 1993. Displacement history of the Atacama fault system 25°00′ S-27°00′ S, northern Chile. Geological Society of America Bulletin 105(9): 1165-1174. https://doi.org/10.1130/0016-7606(1993)105<1165:DHOTAF>2.3.CO;2

Cao, W.; Zahirovic, S.; Flament, N.; Williams, S.; Golonka, J.; Müller, R. D. 2017. Improving global paleogeography since the late Paleozoic using paleobiology. *Biogeosciences*, *14*(23), 5425-5439.

Clarke, L. J., and Jenkyns, H. C. 1999. New oxygen isotope evidence for long-term Cretaceous climatic change in the Southern Hemisphere. *Geology*, *27*(8), 699-702.

Coira, B.; Davidson, J.; Mpodozis, C.; Ramos, V.A. 1982. Tectonic and magmatic evolution of the Andes of northern Argentina and Chile. Earth-Science Reviews 18 (3-4): 303-332. doi: https://doi.org/10.1016/0012-8252(82)90042-3.

Creixell, C.; Labbé, M.; Arévalo, C.; Salazar, E. 2013. Geología del área Estación Chañar-Junta de Chingoles, Regiones de Atacama y Coquimbo. Servicio Nacional de Geología y Minería, Carta Geológica Chile, Serie Geología Básica 150: 85 p., 1 mapa escala 1:1100.000. Santiago.

Creixell, C., Oliveros, V., Vásquez, P., Navarro, J., Vallejos, D., Valin, X., Godoy, E., N. Ducea, M., 2016. Geodynamics of Late Carboniferous-Early Permian forearc in north Chile (28°30′-29°30′S). Journal of the Geological Society 173 (5): 757-772. https://doi.org/10.1144/jgs2016-010

Creixell, C.; Ortiz, M.; Arévalo, C. 2012. Geología del área Carrizalillo-El Tofo, Región de Atacama y Coquimbo. Servicio Nacional de Geología y Minería, Carta Geológica de Chile, Serie Geología Básica 133-134: 82 p., 1 mapa escala 1:100.000. Santiago.

Creixell, C.; Fuentes, J.; Bierma, H.; Salazar, E. 2020. Tectonic setting of Cretaceous porphyry copper deposits of northern Chile (28°-30° S) and its relations with magmatic evolution and metallogeny. Andean Geology 47 (3): 469-507. doi: http://dx.doi.org/10.5027/andgeoV47n3-3035

Dediós, P. 1967. Cuadrángulo Vicuña, Provincia de Coquimbo. Instituto de Investigaciones

Del Real, I.; Allmendinger, R.W.; Thompson, J.F.; Creixell, C. 2023. Evidence for transpression during formation of the Candelaria Punta del Cobre IOCG-district and regional implications. Journal of South American Earth Sciences 126. https://doi.org/10.1016/j.jsames.2023.104289

Emparán, C.; Pineda, G., 1999. Área Condoriaco-Rivadavia, Región de Coquimbo. Servicio Nacional de Geología y Minería, Mapas Geológicos 12, 1 mapa escala 1:100.000. Santiago.

Emparán, C., Pineda, G., 2000. Área La Serena–La Higuera, Región de Coquimbo, escala 1:100.000. Mapas Geológicos, No. 18. Servicio Nacional de Geología y Minería, Santiago.

Engelke, J.; Esser, K.J.; Linnert, C.; Mutterlose, J.; Wilmsen, M. 2016. The benthic macrofauna from the Lower Maastrichtian chalk of Kronsmoor (northern Germany, Saturn quarry): taxonomic outline and palaeoecologic implications. Acta Geologica Polonica.

Folguera, A., Ramos, V.A., 2011. Repeated eastward shifts of arc magmatism in the Southern Andes: A revision to the long-term pattern of Andean uplift and magmatism. *Journal of South American Earth Sciences* 32, 531–546. https://doi.org/10.1016/j.jsames.2011.04.003

Foreman, B. Z.; Heller, P. L.; Clementz, M. T. 2012. Fluvial response to abrupt global warming at the Palaeocene/Eocene boundary. *Nature*, *491*(7422), 92-95.

Friedrich, O.; Norris, R.D.; Erbacher, J. 2012. Evolution of middle to Late Cretaceous oceans—A 55 m.y. record of Earth's temperature and carbon cycle. Geology 40 (2): 107-110. https://doi.org/10.1130/G32701.1

González, J.; Oliveros, V.; Creixell, C.; Velásquez, R.; Vásquez, P.; Lucassen, F. 2018. The Triassic magmatism and its relation with the Pre-Andean tectonic evolution: Geochemical and petrographic constrains from the High Andes of north central Chile (29°30'-30° S). Journal of South American Earth Sciences 87: 95-112. https://doi.org/10.1016/j.jsames.2017.12.009

González, J.; Oliveros, V.; Lucassen, F.; Creixell, C.; Coloma, F.; Velásquez, R.; Hernández, L.; Vásquez, P.; Kasemann, S.A. 2025. The Triassic magmatism in southwestern Gondwana: An example of arc batholith construction in a retreating margin. Gondwana Research 139: 81-103. https://doi.org/10.1016/j.gr.2024.12.002

Goudie, A. S. 2006. Global warming and fluvial geomorphology. *Geomorphology*, *79*(3-4), 384-394.

Granot, R.; Dyment, J. 2015. The cretaceous opening of the South Atlantic Ocean. *Earth and Planetary Science Letters*, *414*, 156-163.

Haq, B.U.; Huber, B.T. 2017. Anatomy of a eustatic event during the Turonian (Late Cretaceous) hot greenhouse climate. Science China Earth Sciences 60: 20-29. https://doi.org/10.1007/s11430-016-0166-y

Haq, B.U. 2014. Cretaceous eustasy revisited. Global and Planetary change 113: 44-58. https://doi.org/10.1016/j.gloplacha.2013.12.007

Huber, B.T.; MacLeod, K.G.; Watkins, D.K.; Coffin, M.F. 2018. The rise and fall of the Cretaceous Hot Greenhouse climate. Global and Planetary Change 167: 1-23. https://doi.org/10.1016/j.gloplacha.2018.04.004

Iannelli, S.B.; Fernández Paz, L.; Litvak, V.D.; Gianni, G.; Fennell, L.M.; González, J.; Lucassen, F.; Kasemann, S.; Oliveros, V.; Folguera, A. 2020. Southward-directed subduction of the Farallon-Aluk spreading ridge and its impact on subduction mechanics and Andean arc magmatism: Insights from geochemical and seismic tomographic data. Frontiers in Earth Science 8. https://doi.org/10.3389/feart.2020.00121

Jaillard, E.; Bengtson, P.; Dhondt, A. V. 2005. Late Cretaceous marine transgressions in Ecuador and northern Peru: a refined stratigraphic framework. *Journal of South American Earth Sciences*, *19*(3), 307-323.

Lossada, A. C., Giambiagi, L., Hoke, G. D., Fitzgerald, P. G., Creixell, C., Murillo, I., Mardonez, D., Velásquez, R., Suriano, J. 2017. Thermochronologic evidence for late Eocene Andean mountain building at 30 S. *Tectonics*, *36*(11), 2693-2713.

Maksaev, V.; Munizaga, F.; Valencia, V.; Barra, F. 2009. LA-ICP-MS zircon U-Pb geochronology to constrain the age of post-Neocomian continental deposits of the Cerrillos Formation, Atacama Region, northern Chile: tectonic and metallogenic implications. Andean Geology 36 (2): 264-287. https://dx.doi.org/10.5027/andgeoV36n2-a05

Maksaev, V.; Munizaga, F.; Tassinari, C. 2014. Timing of the magmatism of the paleo-Pacific border of Gondwana: U-Pb geochronology of Late Paleozoic to Early Mesozoic igneous rocks of the north Chilean Andes between 20° and 31 °S. Andean Geology 41 (3): 447-506. https://dx.doi.org/10.5027/andgeoV41n3-a01

Martin, M.W.; Clavero, J.; Mpodozis, C. 1999. Late paleozoic to early jurassic tectonic development of the high andean principal cordillera, el indio region, Chile (29-30 °S). Journal of South American Earth Sciences 12 (1): 33-49. https://doi.org/10.1016/S0895-9811(99)00003-6

Martínez, F.; Arriagada, C.; Mpodozis, C.; Peña, M. 2012. The Lautaro Basin: A record of inversion tectonics in northern Chile. Andean Geology 39 (2): 258-278. https://dx.doi.org/10.5027/andgeoV39n2-a04

Martínez, F.; Arriagada, C.; Peña, M.; Del Real, I.; Deckart, K. 2013. The structure of the Chañarcillo Basin: An example of tectonic inversion in the Atacama region, northern Chile. *Journal of South American Earth Sciences*, *42*, 1-16.

Merino, R. 2013. Estratigrafía, sedimentología y proveniencia de las sucesiones continentales de tras-arco del Jurásico Superior, entre los 28°30'–30°S y 69°50'–70°40'W. Undergraduate Thesis (Unpublished), Departamento de Geociencias, Universidad de Concepción: 111 p.

Merino, R.; Salazar, E.; Mora-Franco, C.; Creixell, C.; Coloma, F.; Oliveros, V. 2013. Fluvial deposition and retro-arc volcanism in a Late Cretaceous foreland basin and the unroofing of the Early Cretaceous arc in the chilean Frontal Cordillera at 28°30' S, Atacama Region. Bolletino di Geofisica teorica ed applicata 54: 237-238.

Moscoso, R.; Mpodozis, C. 1988. Estilos estructurales en el norte chico de Chile (28-31°S), regiones de Atacama y Coquimbo. Revista Geológica de Chile 15: 151-166.

Mourgues, A. 2001. Bioestratigrafía y paleontología del Grupo Chañarcillo, Cretácico Inferior, III Región, Chile (Inédito), Servicio Nacional de Geología y Minería, Informe Paleontológico. No. 2000-09, 84 p.

Mpodozis, C.; Cornejo, P. 1988. Hoja Pisco Elqui, IV Región de Coquimbo. Servicio Nacional de Geología y Minería, Carta Geológica de Chile 68: 164 p. , 1 mapa escala 1:250.000. Santiago.

Mpodozis, C.; Ramos, V. 1990. The Andes of Chile and Argentina. Chapter 5. *In* Geology of the Andes and its relation to hydrocarbon and mineral resources (Ericksen, G.E.; Cañas Pinochet, M.T.; Reinemund, J.A.; editors). Circum-Pacific Council for Energy and Mineral Resources Earth Science Series 11: 59-90. Houston.

Muñoz, N.; Jordan, T.E.; Charrier, R. 2002. Interactions between basement and cover during the evolution of the Salar de Atacama basin, northern Chile. Revista Geológica de Chile 29: 55-80.

Murillo, I.; Velásquez, R.; Creixell, C. 2017. Geología de las áreas Guanta-Los Cuartitos y Paso de Vacas Heladas, regiones de Atacama y Coquimbo. Servicio Nacional de Geología y Minería, Carta Geológica Chile, Serie Geología Básica 192-193: 96 p., 1 mapa escala 1:100.000. Santiago.

Müller, R.D.; Seton, M.; Zahirovic, S.; Williams, S.E.; Matthews, K.J.; Wright, N.M.; Shephard, G.; Maloney, K.; Barnett-Moore, N.; Hosseinpour, M.; Bower, D.; Cannon, J. 2016. Ocean basin evolution and global-scale plate reorganization events since Pangea breakup. Annual Review of Earth and Planetary Sciences 44 (1): 107-138. https://doi.org/10.1146/annurev-earth-060115-012211

Müller, R. D.; Zahirovic, S.; Williams, S. E.; Cannon, J.; Seton, M.; Bower, D. J.; Tetley, M. G.; Heine, C.; Le Breton, E.; Liu, S.; Russel, S. H. J.; Yang, T.; Leonard, J.; Gurnis, M. 2019. A global plate model including lithospheric deformation along major rifts and orogens since the Triassic. *Tectonics*, *38*(6), 1884-1907.

Oliveros, V.; González, J.; Espinoza Vargas, M.; Vásquez, P.; Rossel, P.; Creixell, C.; Sepúlveda, F.; Bastias, F. 2018. The Early Stages of the Magmatic Arc in the Southern Central Andes. *In* The Evolution of the Chilean-Argentinean Andes (Folguera, A.; Contreras-Reyes, E.; Heredia, N.; Encinas, A.; Iannelli, S.B.; Oliveros, V.; Dávila, F.M.; Collo, G.;

Giambiagi, L.; Maksymowicz, A.; Iglesia Llanos, M.P.; Turienzo, M.; Naipauer, M.; Orts, D.; Litvak, V.D.; Alvarez, O.; Arriagada, C.; editors). Springer International Publishing: 165-190. Cham. https://doi.org/10.1007/978-3-319-67774-3_7

Ortiz, M.; Merino, R.N. 2015. Geología de las áreas Río Chollay-Matancilla y Cajón del Encierro, regiones de Atacama y Coquimbo. Servicio Nacional de Geología y Minería, Carta Geológica Chile, Serie Geología Básica 175-176: 234 p., 1 mapa escala 1:100.000. Santiago.

Rivano, S., Sepúlveda, P., Boric, R., Espiñeira, D., 1993. *Hojas Quillota y Portillo*, escala 1:250.000. Carta Geológica de Chile, No. 73. Servicio Nacional de Geología y Minería, Santiago.

Rodríguez, M.P.; Aguilar, G.; Urresty, C.; Charrier, R. 2015. Neogene landscape evolution in the Andes of north-central Chile between 28 and 32 S: interplay between tectonic and erosional processes. *In* Geodynamic Processes in the Andes of Central Chile and Argentina (Sepúlveda, S.A.; Giambiagi, L.B.; Moreiras, S.M.; Pinto, L.; Tunik, M.; Hoke, G.D.; Farías, M.; editors). Geological Society, London, Special Publications. London. https://doi.org/10.1144/SP399.15

Rodríguez, M. P., Charrier, R., Brichau, S., Carretier, S., Farías, M., de Parseval, P., Ketcham, R. A. 2018. Latitudinal and longitudinal patterns of exhumation in the Andes of north-central Chile. *Tectonics*, *37*(9), 2863-2886.

Rossel, K.; Aguilar, G.; Salazar, E.; Martinod, J.; Carretier, S.; Pinto, L.; Cabré, A. 2016. Chronology of Chilean Frontal Cordillera building from geochronological, stratigraphic and geomorphological data: Insights from Miocene intramontane-basin deposits. Basin Research 30: 289-310. doi: 10.1111/bre.12221.

Roux, M.; Cahuzac, B.; Sztrákos, K. 2006. Les paléoenvironnements éocènes à crinoïdes pédonculés des marnes de Miretrain (Angoumé, SW France): interprétations paléobathymétriques. Comptes Rendus Géoscience, 338(4): 262–271.

Roux, M.; Martinez-Soares, P.; Fornaciari, E.; Gatto, R.; Papazzoni, C.A.; Giusberti, L. 2024. Eocene stalked crinoids in the genus Isselicrinus (Echinodermata, Crinoidea, Isocrinida) from northeastern Italy. Rivista Italiana di Paleontologia e Stratigrafia, 130(1).

Salazar, E.; Coloma, F. 2016. Geología del área Cerros de Cantaritos-Laguna Chica, Región de Atacama. Servicio Nacional de Geología y Minería, Carta Geológica Chile, Serie Geología Básica 181: 171 p., 1 mapa escala 1:100.000. Santiago.

Salazar, E.; Coloma, F.; Creixell, C. 2013. Geología del área El Tránsito-Lagunillas, Región de Atacama. Servicio Nacional de Geología y Minería, Carta Geológica Chile, Serie Geología Básica 149: 106 p., 1 mapa escala 1:100.000. Santiago.

Salazar Pérez, E.F. 2012. Evolución tectono-estratigráfica post-paleozoica de la cordillera de Vallenar. Tesis de Magíster (Inédito), Universidad de Chile, Facultad de Ciencias Físicas y Matemáticas, Departamento de Geología: 126 p.

Salazar, E.; Vásquez, P.; Vallejos, D.; Creixell, C.; Oliveros, V.; Ducea, M. 2020. Stratigraphic and provenance analysis of Triassic rock units between 28-29° S, northern Chile:

implications on the tectonic and paleogeographic evolution of the southwestern margin of Gondwana. Andean Geology 47 (2): 207-255. https://dx.doi.org/10.5027/andgeoV47n2-3118

Segerstrom, K.; Parker, R.L. 1959. Cuadrángulo Cerrillos, Provincia de Atacama. Instituto de Investigaciones Geológicas, Carta Geológica de Chile 2: 33 p., 1 mapa escala 1:50.000. Santiago.

Somoza, R.; Ghidella, M.E. 2012. Late Cretaceous to recent plate motions in western South America revisited. Earth and Planetary Science Letters 331-332: 152-163. https://doi.org/10.1016/j.epsl.2012.03.003

Tunik, M.A.; Álvarez, P. 2008. Análisis y edad de la sección calcárea de la Formación Las Chilcas (Chile) y sus implicancias para la correlación con unidades de Argentina. Revista de la Asociación Geológica Argentina, 63 (3): 363-379.

van der Meer, D.G.; Scotese, C.R.; Mills, B.J.; Sluijs, A.; van de Weg, R.M. 2022. Long-term Phanerozoic global mean sea level: insights from strontium isotope variations and estimates of continental glaciation. Gondwana Research 111: 103–121.

Wall, R., Selles, D., Gana, P., 1999. *Área Tiltil–Santiago, Región Metropolitana*, escala 1:100.000. Carta Geológica de Chile, No. 39. Servicio Nacional de Geología y Minería, Santiago.

Wang, Y.; Huang, C.; Sun, B.; Quan, C.; Wu, J.; Lin, Z. 2014. Paleo-CO2 variation trends and the Cretaceous greenhouse climate. Earth-Science Reviews 129: 136-147.

Welkner, D.; Arévalo, C.; Godoy P, E. 2006. Geología del área Freirina-El Morado, Región de Atacama. Servicio Nacional de Geología y Minería. Carta Geológica de Chile, Serie Geología Básica 100: 50 P., 1 mapa escala 1:100.000. Santiago.

Willner, A.P.; Gerdes, A.; Massonne, H.J. 2008. History of crustal growth and recycling at the Pacific convergent margin of South America at latitudes 29°-36° S revealed by a U-Pb and Lu-Hf isotope study of detrital zircon from late Paleozoic accretionary systems. Chemical Geology 253 (3-4): 114-129. https://doi.org/10.1016/j.chemgeo.2008.04.016

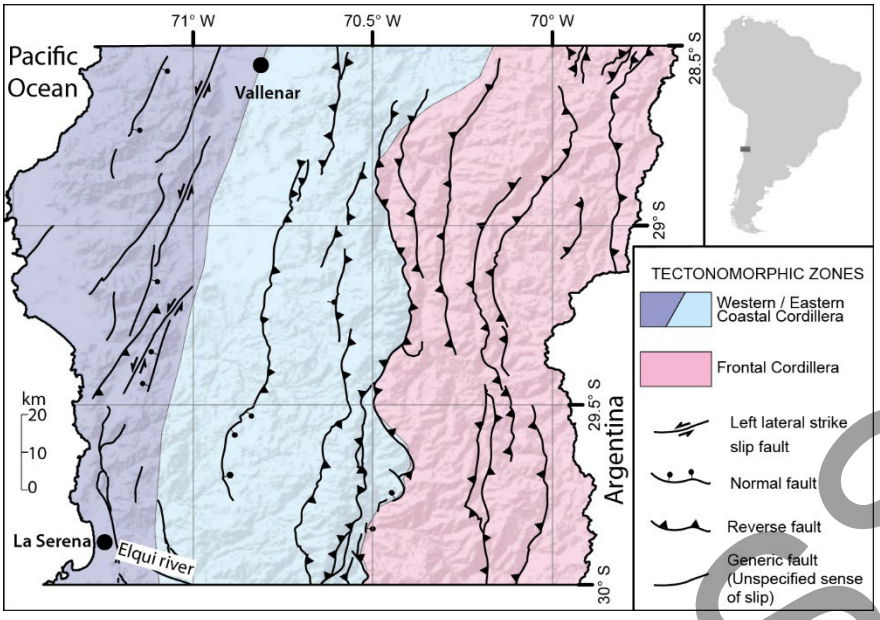

Fig. 1. Main tectonomorphic zones (colored areas) and tectonic structures in the 28.5-30° S Chilean segment of the Andes. Main cities are shown as black circles.

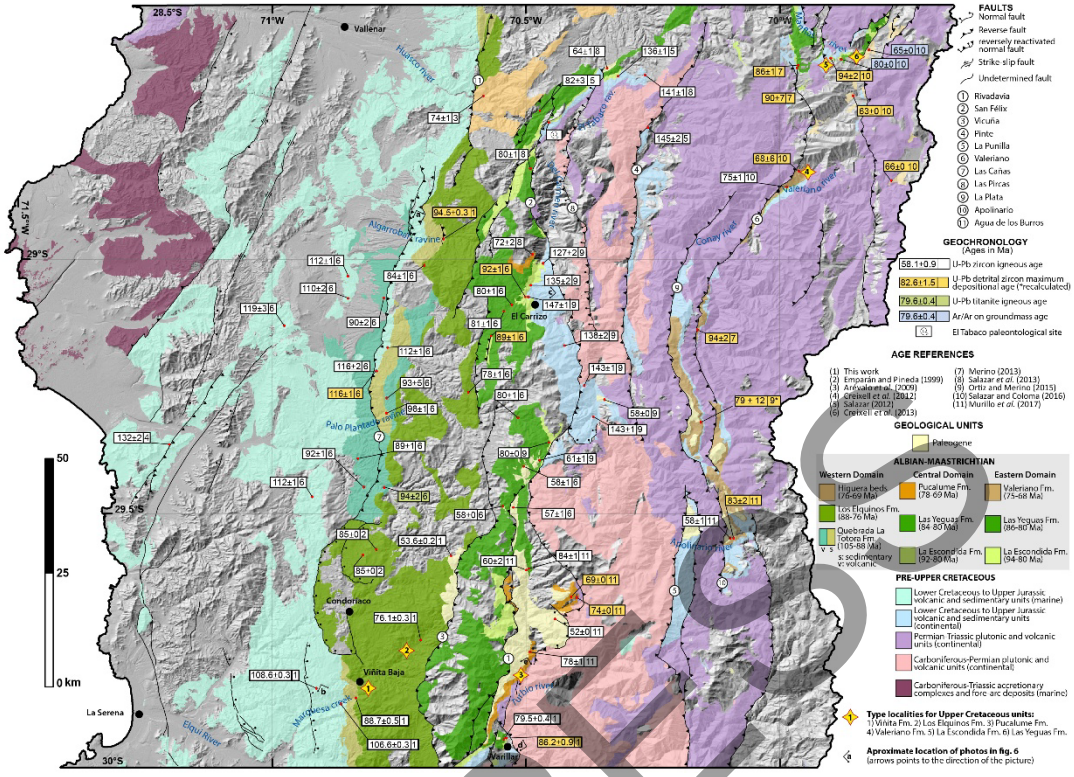

Fig. 2. Geological map of the study area, showing stratified Cretaceous rocks. Black circles refer to main towns and cities. Former Quebrada La Totora beds and La Escondida and Las Yeguas members are referred to as formations after this work (see text for more details). All ages are listed in Supplementary Table 1

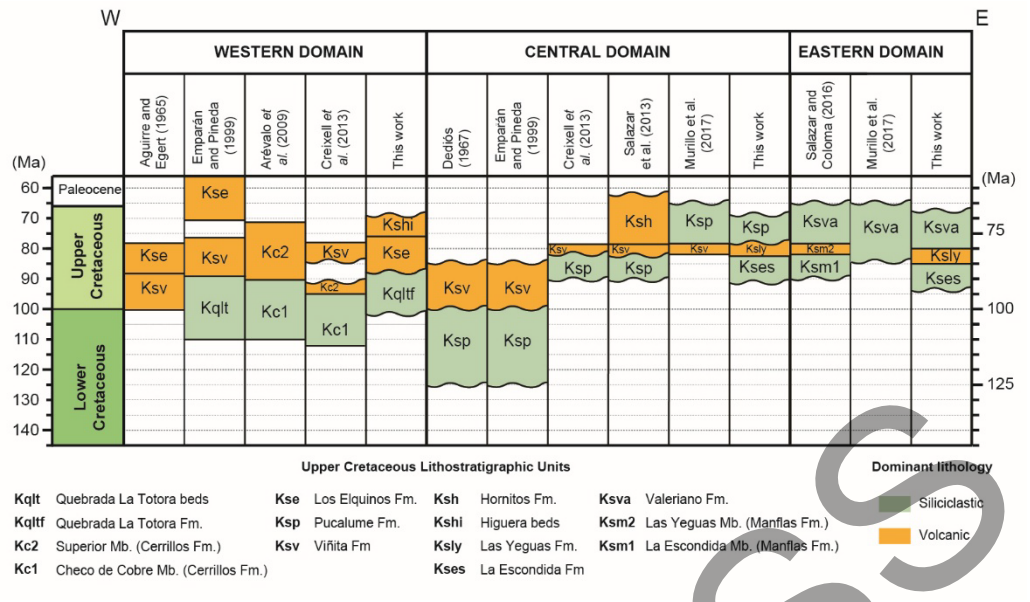

Fig. 3. Summary of Upper Cretaceous stratigraphic nomenclature available in the literature for the 28.5-30° S segment.

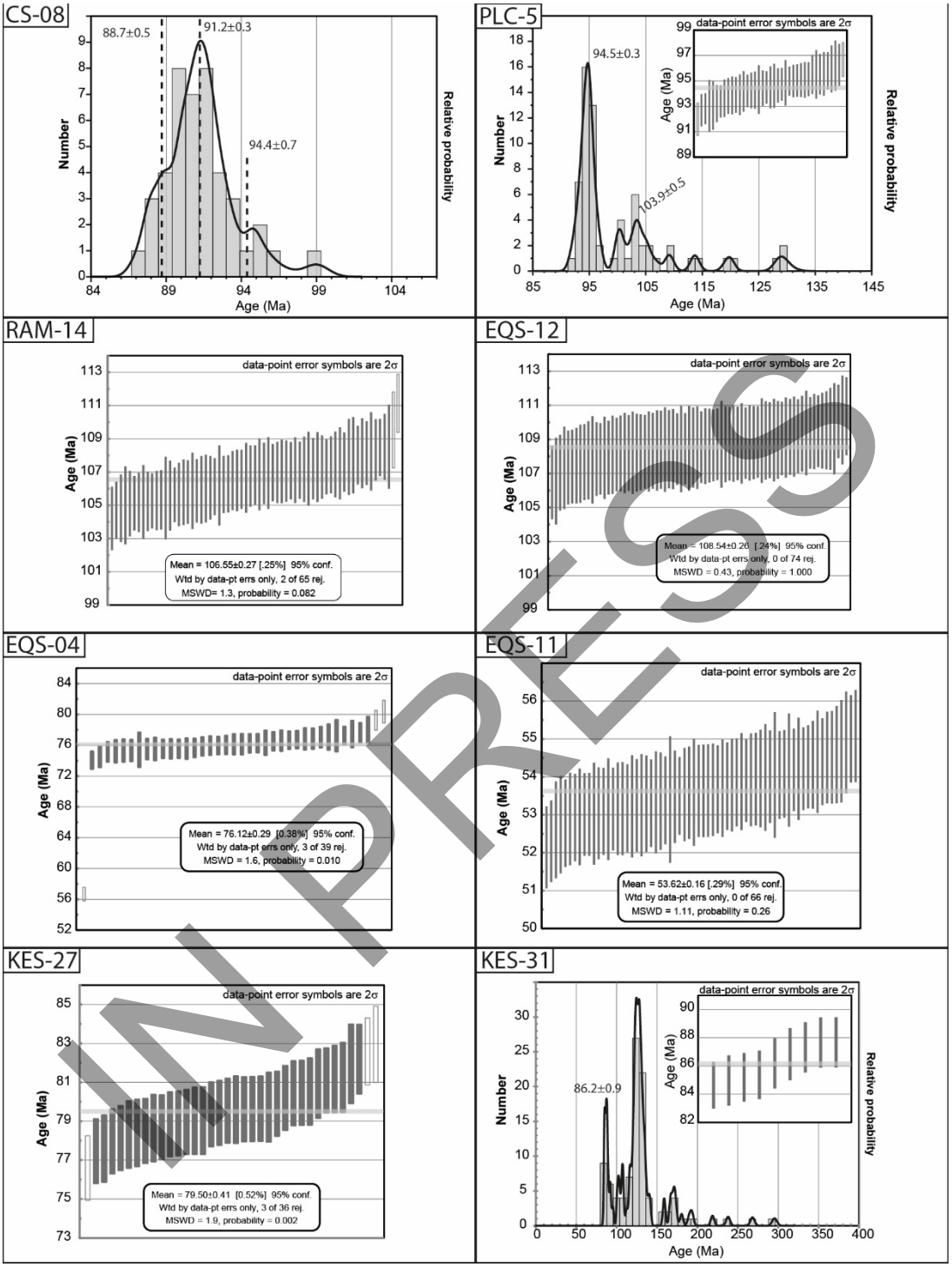

Fig. 4. U-Pb age diagrams from this study. Density probability plots for samples CS-08, PLC-5 and KES-31, and weighted means calculated for samples RAM-14, EQS-04, EQS-11, EQS-12, KES-27 and KES-31 (data point errors at the 2σ model range). Details

of the calculation of each age are provided in Section 3.2 and in Supplementary Table 2. Wtd = weighted, data-pt = data-points, rej = rejected, MSWD = Mean Square Weighted Deviation.

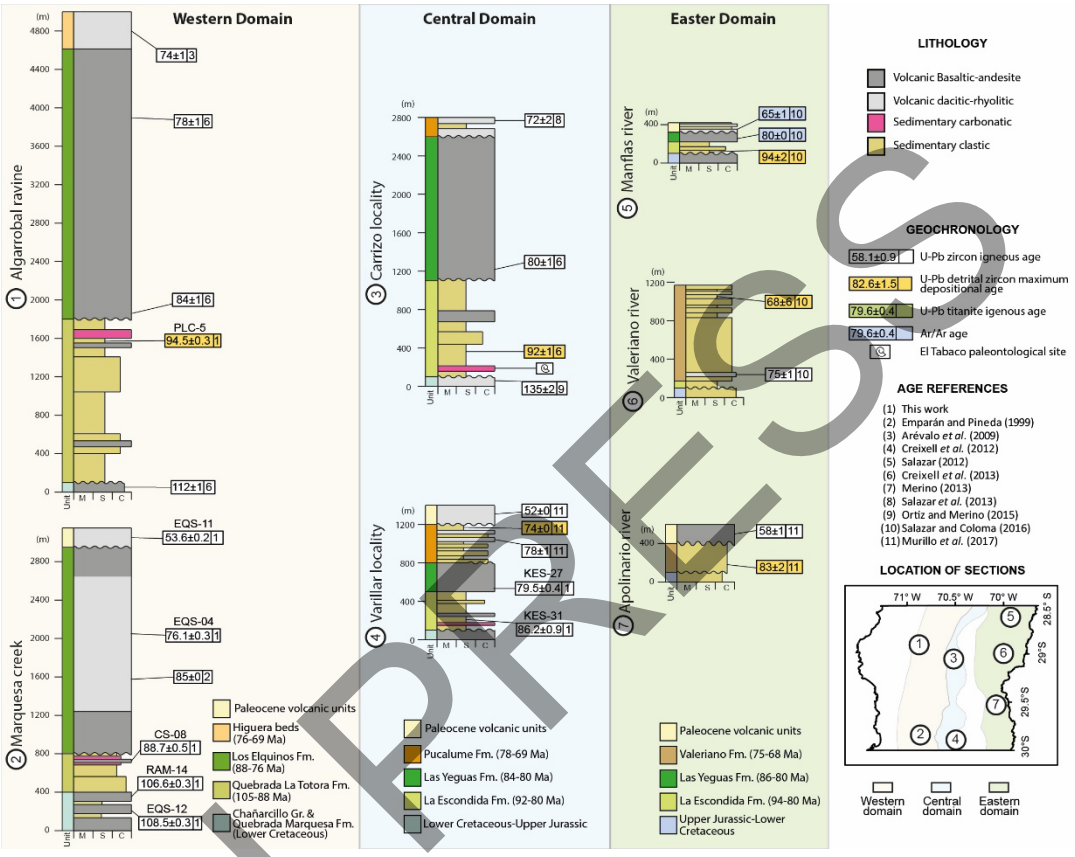

Fig. 5. Synthetic stratigraphic columns for Cretaceous units in the three stratigraphic domains defined in this study. Column thicknesses in meters. See figure 2 for comparisons and spatial context. M = Mudstone; S = Sandstone; C = Conglomerate.

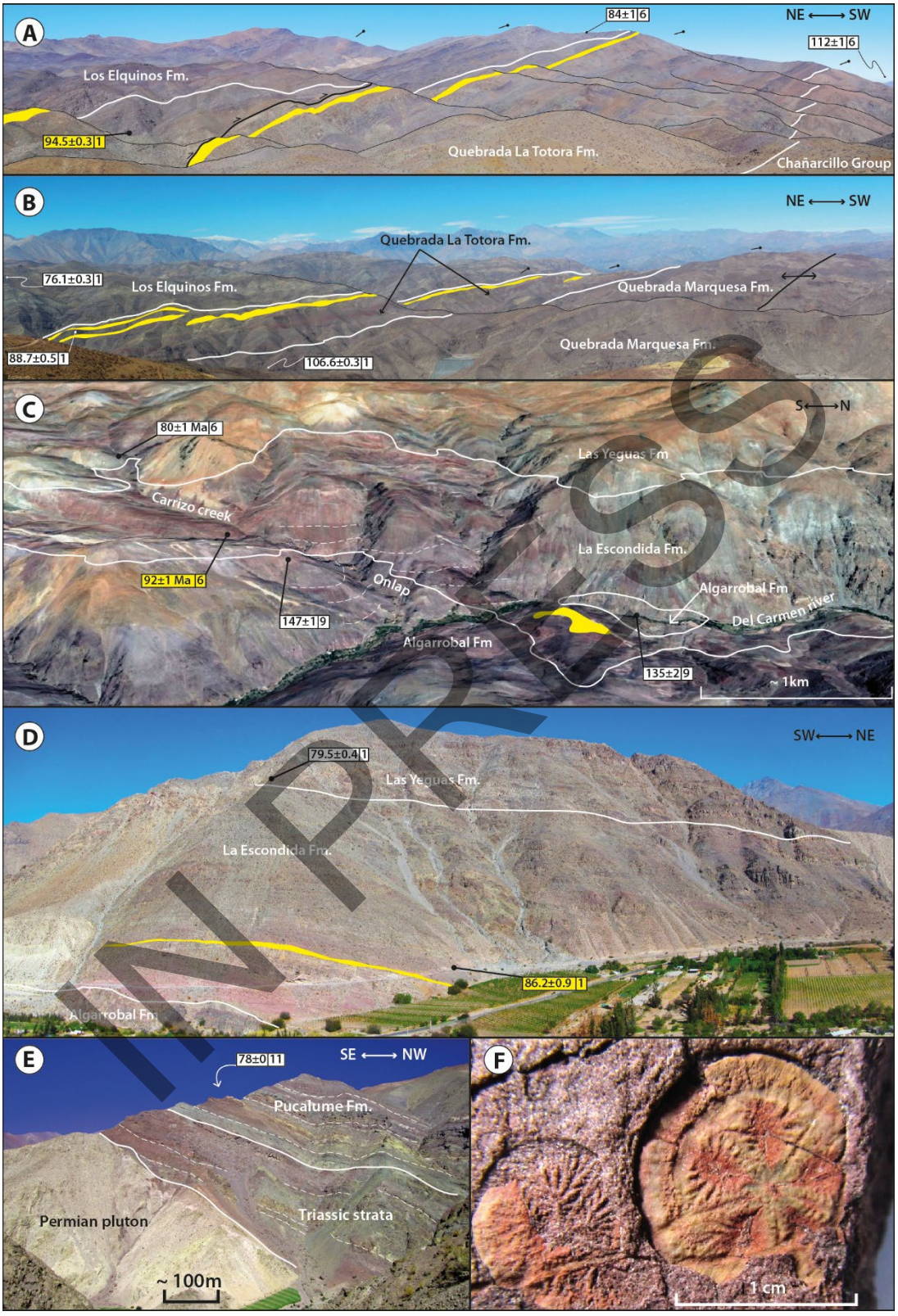
A
NE ⟷ SW
84±1 6
112±1 6
Los Elquinos Fm.
94.5±0.3 1
Quebrada La Totora Fm.
Chañarcillo Group
B
NE ⟷ SW
Quebrada La Totora Fm.
76.1±0.3 1
Los Elquinos Fm.
Quebrada Marquesa Fm.
Quebrada Marquesa Fm.
88.7±0.5 1
106.6±0.3 1
C
S ⟷ N
80±1 Ma 6
Las Yeguas Fm
Carrizo creek
La Escondida Fm.
92±1 Ma 6
Onlap
Algarrobal Fm
Del Carmen river
147±1 9
Algarrobal Fm
135±2 9
~ 1km
D
SW ⟷ NE
79.5±0.4 1
Las Yeguas Fm.
La Escondida Fm.
86.2±0.9 1
Algarrobal Fm
E
SE ⟷ NW
78±0 11
Pucalume Fm.
Permian pluton
Triassic strata
~ 100m
F
1 cm

Fig. 6. Field photographs of key stratigraphic features from Cretaceous units along the study area. **A.** Western Domain, Algarrobal ravine area. Thick black line with arrows shows reverse fault. **B.** Western Domain, Marquesa creek area. **C.** Central Domain, El Carrizo locality, where the La Escondida Formation onlaps onto the eroded Algarrobal Formation. **D.** Central Domain, Varillar locality. **E.** Central Domain, north of Varillar locality. **F.** Central Domain, *Isselicrinus*? sp. fossils from the La Escondida Formation. Yellow swaths enclose carbonate strata. Thick, solid white lines show stratigraphic contacts. Thin, segmented white lines show stratification. Age references same as in figures 2 and 5. Panel C from Google Earth.

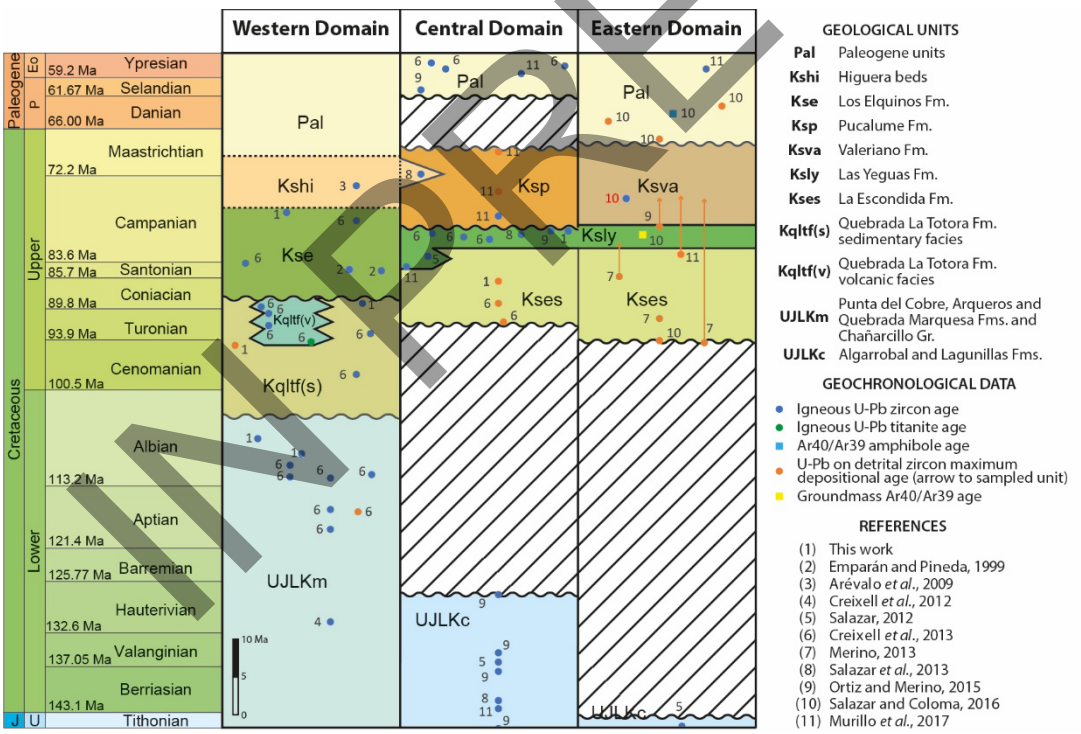

Fig. 7. New chronostratigraphic framework for the Cretaceous units between 28.5-30° S.

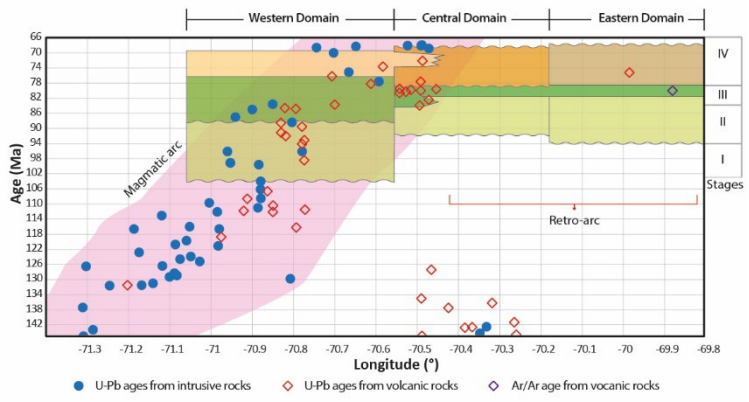

Fig. 8. East-west distribution of arc magmatism-related U-Pb and Ar/Ar ages published in the studied area (see text for references), and relative east-west distribution of studied Upper Cretaceous units described in this work for each domain (color code same as in figures 2 and 7). Arc magmatism is outlined in pink, of which an eastward progression is evident. Geochemical analysis on Upper Cretaceous volcanic and subvolcanic rocks outcropping in the western and central domains show consistently arc-related signatures and mineralization style (Creixell *et al.*, 2020). These features suggest that the Western Domain was completely developed in an intra-arc context, while the Central Domain evolved from a retro-arc to an intra-arc position and the Eastern Domain stayed in a retro-arc position throughout the Late Cretaceous, hosting only discrete magmatic activity.

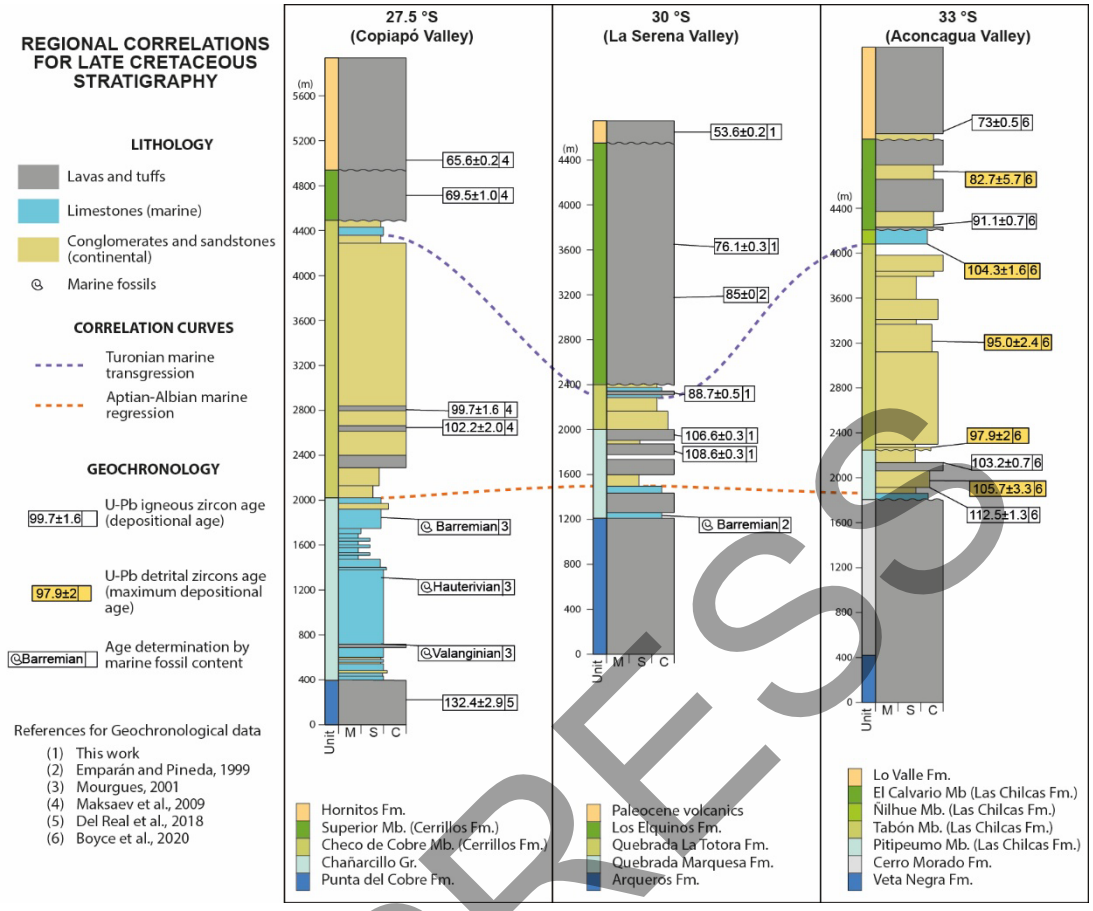

FIG. 9. Regional comparison between Cretaceous stratified units in the Coastal Cordillera of north-central Chile between 27.5 and 33° S. Note the regional nature of Albian continental clastic and Turonian marine limestone deposition. M = Mudstone; S = Sandstone; C = Conglomerate.

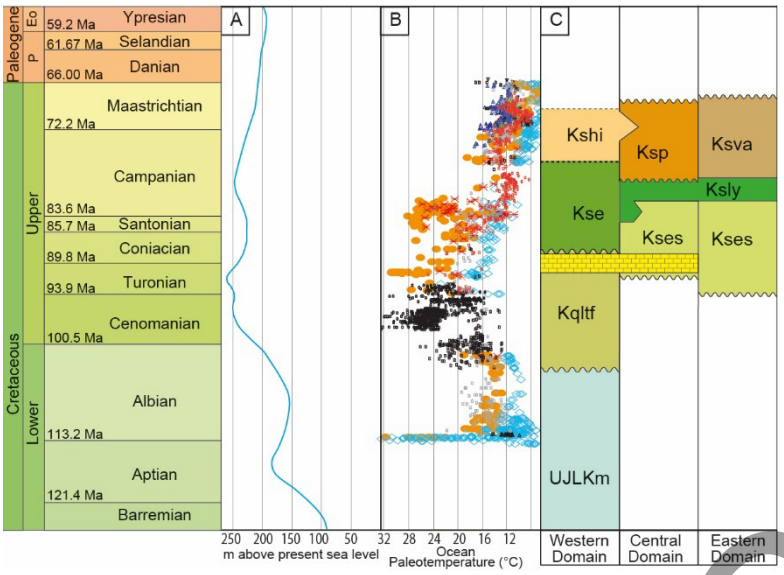

Fig. 10. Comparison of global oceanic events with local stratigraphy for the Aptian-Thanetian. **A.** Global eustatic curve after Haq (2014). **B.** Ocean paleotemperature data from isotopic analysis of benthic and planktonic foraminifers compiled by Friedrich *et al.* (2012) and Huber *et al.* (2018). Black squares and triangles: North Atlantic (benthic). Gray squares: Southern high latitudes (benthic). Red squares: Pacific Ocean (benthic). Blue triangles: Subtropical South Atlantic (benthic). Green squares: Indian Ocean (benthic). Orange circles: South Atlantic and South Indian oceans (planktonic). Light blue diamonds: South Atlantic and South Indian oceans (benthic). Red asterisks: South Atlantic and South Indian oceans (deep planktonic). **C.** Local stratigraphy from this study, as in figure 7. Yellow band shows carbonate intervals in the Western and Central domains.

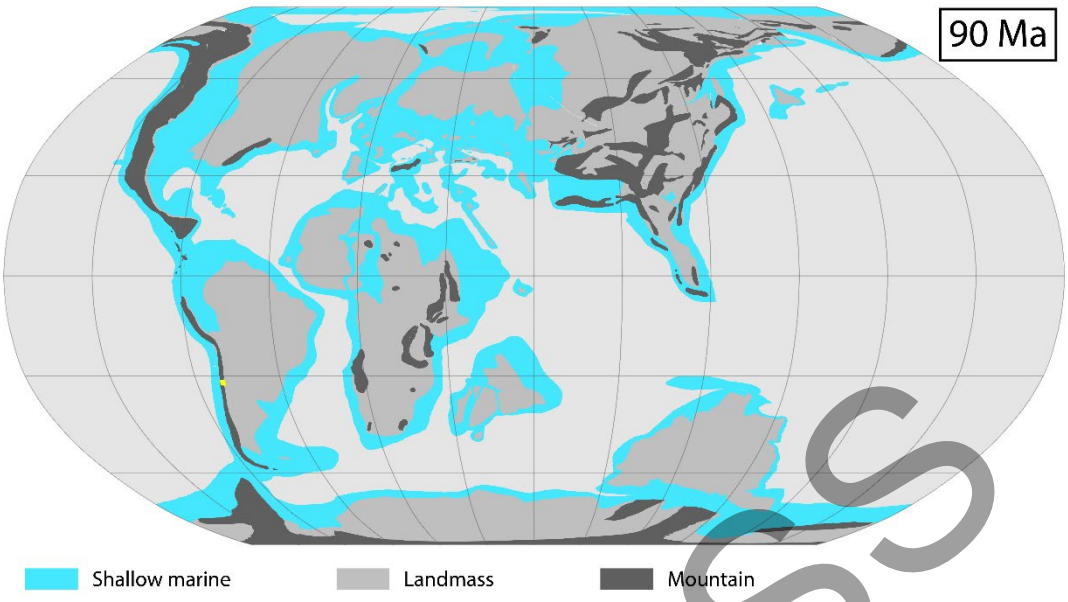

Fig. 11. Worldwide shallow seas distribution at ~90 Ma after Cao *et al.* (2017). Yellow zone indicates the location of the study area. (No data from northern Chile were considered for this reconstruction.)

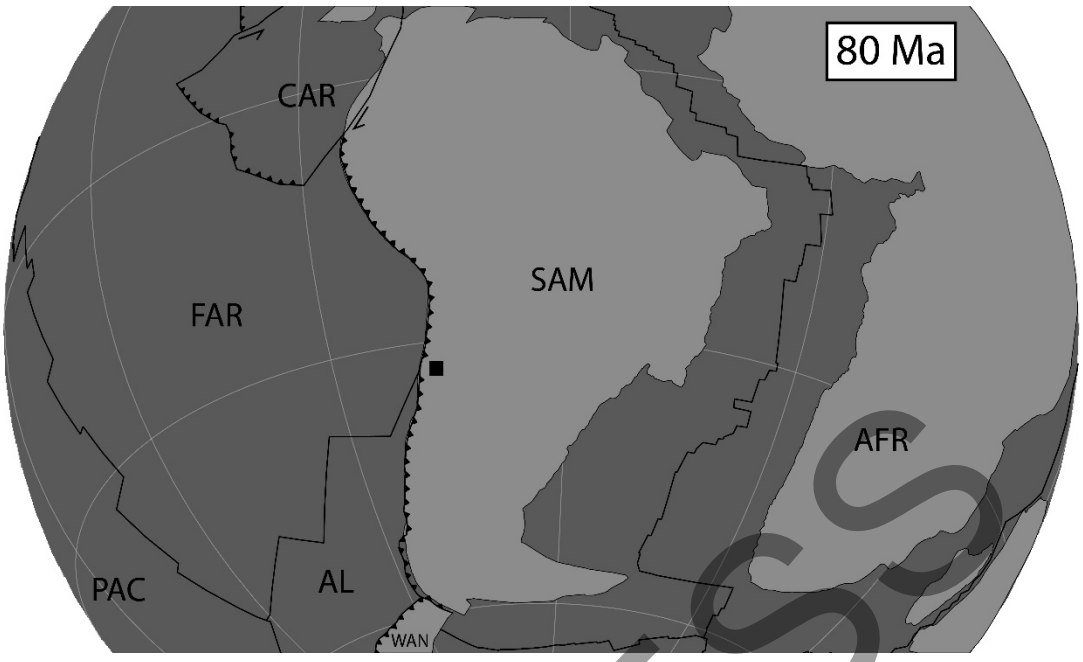

Fig. 12. Tectonic plate reconstruction at ~80 Ma for South America according to Müller *et al.* (2019). The black square shows the location of the study area. SAM: South American plate; FAR: Farallon plate; AL: Aluk plate; PAC: Pacific plate; CAR: Caribbean plate; AFR: African plate; WAN: West Antarctic plate.